



# RESEARCH MEMORANDUM

AERODYNAMIC CHARACTERISTICS AT SUPERSONIC SPEEDS OF A  
SERIES OF WING-BODY COMBINATIONS HAVING CAMBERED  
WINGS WITH AN ASPECT RATIO OF 3.5 AND A  
TAPER RATIO OF 0.2

EFFECTS OF SWEEP ANGLE AND THICKNESS RATIO ON THE STATIC  
LATERAL STABILITY CHARACTERISTICS AT  $M = 1.60$

By M. Leroy Spearman and John H. Hilton, Jr.

Langley Aeronautical Laboratory  
Langley Field, Va.

NATIONAL ADVISORY COMMITTEE  
FOR AERONAUTICS  
WASHINGTON

January 21, 1952  
Declassified May 16, 1958

NATIONAL ADVISORY COMMITTEE FOR AERONAUTICS

RESEARCH MEMORANDUM

AERODYNAMIC CHARACTERISTICS AT SUPERSONIC SPEEDS OF A  
SERIES OF WING-BODY COMBINATIONS HAVING CAMBERED  
WINGS WITH AN ASPECT RATIO OF 3.5 AND A  
TAPER RATIO OF 0.2

EFFECTS OF SWEEP ANGLE AND THICKNESS RATIO ON THE STATIC  
LATERAL STABILITY CHARACTERISTICS AT  $M = 1.60$

By M. Leroy Spearman and John H. Hilton, Jr.

SUMMARY

An investigation has been conducted in the Langley 4- by 4-foot supersonic pressure tunnel at a Mach number of 1.60 and a Reynolds number of  $2.7 \times 10^6$ , based on the wing mean aerodynamic chord, to determine the effects of sweep angle and thickness ratio on the static lateral stability characteristics of a series of wing-body combinations having cambered wings of aspect ratio 3.5 and taper ratio 0.2. The wings, tested on a body of revolution, had quarter-chord sweep angles of  $10.8^\circ$ ,  $35^\circ$ , and  $47^\circ$  with a thickness ratio of 4 percent, and thickness ratios of 4, 6, and 9 percent with a sweep angle of  $47^\circ$ . The effects of a nacelle installation on the 6-percent-thick  $47^\circ$  swept wing were also investigated. The results of these tests show the effects of sweep, thickness, and the nacelle installation on the static lateral stability characteristics.

INTRODUCTION

A research program has been in progress at the Langley Aeronautical Laboratory to determine at subsonic, transonic, and supersonic speeds, the effects of thickness and sweep on the aerodynamic characteristics of a series of wing-body combinations with cambered wings having a taper ratio of 0.2 and an aspect ratio of 3.5. The effects of thickness on the longitudinal characteristics of a  $47^\circ$  sweepback wing-body combination at subsonic and transonic speeds are presented in reference 1. The

effects of sweep and thickness on the longitudinal characteristics for the series of wings at a Mach number of 1.60 are presented in reference 2. The results of tests of several nacelle installations on a  $47^{\circ}$  sweptback wing are presented in reference 3.

As a part of this research program, the present paper reports the results of an investigation made to determine some effects of sweep and thickness on the static lateral stability characteristics of this series of wing-body combinations at a Mach number of 1.60 and a Reynolds number of  $2.7 \times 10^6$  based on the wing mean aerodynamic chord. The wings had quarter-chord sweep angles of  $10.8^{\circ}$ ,  $35^{\circ}$ , and  $47^{\circ}$  with a thickness ratio of 4 percent, and thickness ratios of 4, 6, and 9 percent with a sweep angle of  $47^{\circ}$ . In addition, the effects of a nacelle installation on the 6-percent-thick  $47^{\circ}$  sweptback wing were investigated. The results are presented without analysis to expedite issuance.

#### COEFFICIENTS AND SYMBOLS

The results of the tests are presented as standard NACA coefficients of forces and moments. The data are referred to the stability-axes system (fig. 1) with the reference center of gravity at 25 percent of the wing mean aerodynamic chord.

The coefficients and symbols are defined as follows:

$C_Y$	lateral-force coefficient ( $Y/qS$ )
$C_n$	yawing-moment coefficient ( $N/qSb$ )
$C_l$	rolling-moment coefficient ( $L/qSb$ )
$C_L$	lift coefficient ( $-Z/qS$ )
$C_X$	longitudinal-force coefficient ( $X/qS$ )
$C_m$	pitching-moment coefficient ( $M'/qS\bar{c}$ )
$X$	force along X-axis
$Y$	force along Y-axis
$Z$	force along Z-axis
$L$	moment about X-axis

M'	moment about Y-axis
N	moment about Z-axis
q	free-stream dynamic pressure
S	total wing area
b	wing span
$\bar{c}$	wing mean aerodynamic chord
M	Mach number
t/c	thickness ratio (Wing thickness/Wing chord)
$\alpha$	angle of attack of body center line, degrees
$\psi$	angle of yaw, degrees
$\Lambda$	angle of sweep of wing quarter-chord line, degrees
$C_{Y\psi}$	lateral-force parameter, rate of change of lateral-force coefficient with angle of yaw ( $\partial C_Y / \partial \psi$ )
$C_{n\psi}$	directional-stability parameter, rate of change of yawing-moment coefficient with angle of yaw ( $\partial C_n / \partial \psi$ )
$C_{l\psi}$	effective-dihedral parameter, rate of change of rolling-moment coefficient with angle of yaw ( $\partial C_l / \partial \psi$ )

## APPARATUS AND MODELS

## Tunnel

The tests were conducted in the Langley 4- by 4-foot supersonic pressure tunnel. This tunnel, described in reference 4, was originally powered by a 6000-horsepower drive motor. Recent modifications to the tunnel have increased the horsepower rating to 45,000. The additional power has resulted in an increase in the maximum stagnation pressure from 0.3 atmosphere to about 2 atmospheres. The design Mach number range of 1.2 to 2.2 remains unchanged. At a Mach number of 1.60, the test section has a width of 4.5 feet, a height of 4.4 feet, and a region of uniform flow which is 7 feet long at the flexible walls. An external air-drying system supplies air of a sufficiently low dew point to prevent moisture condensation in the test section.

### Models

The models used in these tests were composed of an ogive-cylinder body and various midwing configurations with a ratio of body diameter to wing span of about 0.094. The models were designed to accommodate solid steel wings with integral cylindrical sections simulating corresponding sections of the body. This design permitted interchange of wings with minimum delay. The wings were positioned so that the quarter-chord point of the mean aerodynamic chord was always at the same body station. The wing airfoil sections had an NACA 65A-series thickness distribution with mean line ordinates one-third of NACA 230 plus ( $a = 1$ ) for  $C_L = 0.1$ . The airfoil coordinates are given in table I. Details of the models are shown in figure 2.

The models were sting-supported and had a six-component internal strain-gage balance in the body. The model and sting are shown in figure 3. The models, balance, and indicating systems were furnished by a U. S. Air Force contractor.

### TESTS

#### Test Conditions

The conditions for the tests were:

Mach number . . . . .	1.60
Reynolds number, based on wing mean aerodynamic chord . . . . .	$2.7 \times 10^6$
Stagnation dew point, degrees Fahrenheit . . . . .	<-25
Stagnation pressure, atmosphere . . . . .	1
Stagnation temperature, degrees Fahrenheit . . . . .	110

A limited calibration prior to those tests has shown that the flow in the test section is reasonably uniform. The magnitudes of the variations in the flow parameters are summarized in the following table:

Flow parameter	Magnitude (deg)
Mach number	$\pm 0.01$
Flow angle in horizontal plane	$\pm .1$
Flow angle in vertical plane	$\pm .1$

## Test Procedure

Tests were made through an angle-of-yaw range from  $-2^{\circ}$  to  $10^{\circ}$  at an angle of attack of  $5^{\circ}$  and through an angle-of-attack range from  $-2^{\circ}$  to  $12^{\circ}$  at angles of yaw of  $0^{\circ}$  and  $5^{\circ}$ .

## Corrections and Accuracy

The angles of attack and yaw were corrected for the deflection of the balance under load. The estimated accuracy of both the angle of attack and angle of yaw was  $\pm 0.1^\circ$ . No corrections were applied to the data to account for the flow variations in the test section.

The estimated errors in the force data were as follows:

The base pressure was measured and the drag data were corrected to correspond to a base pressure equal to the free-stream static pressure.

## RESULTS

The results are presented in this paper without analysis in order to expedite publication. The aerodynamic characteristics in yaw for various configurations at  $\alpha = 5^\circ$  are presented in figure 4. The effects of yaw on the lateral characteristics in pitch for various configurations are shown in figure 5. The static lateral stability characteristics of the various configurations at  $\alpha = 5^\circ$  are summarized in table II and are presented as functions of sweep angle and thickness ratio in figure 6.

Although these data are presented without analysis, some general remarks can be made. Both  $C_{Y\Psi}$  and  $C_{n\Psi}$  are essentially invariant with lift coefficient. The effect of increasing the sweep angle or thickness ratio is to increase the positive value of  $C_{Y\Psi}$  and decrease the positive value of  $C_{n\Psi}$ . The effective dihedral  $C_{l\Psi}$ , although quite small, appears to change from negative to positive as the lift coefficient

increases. The effect of the nacelle installation is to increase the positive value of  $C_{Y\psi}$  and  $C_{n\psi}$  and to produce a negative value of  $C_{l\psi}$ .

Langley Aeronautical Laboratory  
National Advisory Committee for Aeronautics  
Langley Field, Va.

REFERENCES

1. Bielat, Ralph P., Harrison, Daniel E., and Coppolino, Domenic A.: An Investigation at Transonic Speeds of the Effects of Thickness Ratio and of Thickened Root Sections on the Aerodynamic Characteristics of Wings with  $47^\circ$  Sweepback, Aspect Ratio 3.5, and Taper Ratio 0.2 in the Slotted Test Section of the Langley 8-Foot High-Speed Tunnel. NACA RM L51I04a, 1951.
2. Robinson, Ross B., and Driver, Cornelius: Aerodynamic Characteristics at Supersonic Speeds of a Series of Wing-Body Combinations Having Cambered Wings with an Aspect Ratio of 3.5 and a Taper Ratio of 0.2. Effects of Sweep Angle and Thickness Ratio on the Aerodynamic Characteristics in Pitch at  $M = 1.60$ . NACA RM L51K16a, 1951.
3. Hasel, Lowell E., and Sevier, John R., Jr.: Aerodynamic Characteristics at Supersonic Speeds of a Series of Wing-Body Combinations Having Cambered Wings with an Aspect Ratio of 3.5 and a Taper Ratio of 0.2. Effect at  $M = 1.60$  of Nacelle Shape and Position on the Aerodynamic Characteristics in Pitch of Two Wing-Body Combinations with  $47^\circ$  Sweptback Wings. NACA RM L51K14a, 1951.
4. Cooper, Morton, Smith, Norman F., and Kainer, Julian H.: A Pressure-Distribution Investigation of a Supersonic Aircraft Fuselage and Calibration of the Mach Number 1.59 Nozzle of the Langley 4- by 4-Foot Supersonic Tunnel. NACA RM L9E27a, 1949.

TABLE I  
AIRFOIL COORDINATES FOR THE VARIOUS WINGS

[Thickness distribution: NACA 65A-series. Mean-line ordinates: one-third of NACA 230 + ( $\alpha = 1$ ) for  $C_L = 0.1$ ]

(a) $\frac{t}{c} = 0.04$			(b) $\frac{t}{c} = 0.06$			(c) $\frac{t}{c} = 0.09$			(d) Thickened root		
x/c	y/c		x/c	y/c		x/c	y/c		x/c	Root station	
	Upper surface	Lower surface		Upper surface	Lower surface		Upper surface	Lower surface		Upper surface	Lower surface
0	0	0	0	0.061	0	0	0.156	0	0	0.301	0
.5	.411	.245	.5	.577	.376	.5	.846	.574	.5	.754	.754
.75	.199	.271	.75	.717	.446	.75	1.021	.680	.75	1.120	.904
1.25	.665	.289	1.25	.919	.534	1.25	1.283	.846	1.25	1.335	1.141
2.5	.962	.324	2.5	1.304	.621	2.5	1.789	1.069	2.5	1.658	1.507
5.0	1.135	.367	5.0	1.872	.761	5.0	2.537	1.400	5.0	2.261	2.024
7.5	1.776	.429	7.5	2.318	.857	7.5	3.111	1.662	7.5	2.008	2.433
10	2.039	.472	10	2.668	.980	10	3.577	1.896	10	4.500	2.799
15	2.123	.577	15	3.150	1.269	15	4.244	2.444	15	5.362	3.445
20	2.642	.682	20	3.482	1.496	20	4.705	2.751	20	5.965	3.984
25	2.800	.787	25	3.701	1.697	25	5.045	3.052	25	6.395	4.414
30	2.897	.892	30	3.858	1.846	30	5.288	3.276	30	6.718	4.716
35	2.983	.997	35	3.946	1.960	35	5.415	3.411	35	6.912	4.910
40	2.992	1.006	40	3.981	2.021	40	5.473	3.529	40	6.977	5.017
45	2.340	1.041	45	3.937	2.030	45	5.424	3.519	45	6.912	4.996
50	2.852	1.006	50	3.823	1.977	50	5.219	3.422	50	6.675	4.823
55	2.712	.945	55	3.613	1.872	55	4.967	3.208	55	6.288	4.522
60	2.511	.857	60	3.342	1.697	60	4.279	2.916	60	5.771	4.113
65	2.265	.761	65	3.018	1.487	65	4.102	2.566	65	5.168	3.618
70	1.986	.674	70	2.651	1.277	70	3.568	2.197	70	4.457	3.101
75	1.680	.577	75	2.231	1.059	75	2.975	1.837	75	3.725	2.584
80	1.356	.481	80	1.785	.849	80	2.382	1.468	80	2.929	2.067
85	1.041	.385	85	1.339	.639	85	1.789	1.098	85	2.239	1.550
90	.726	.289	90	.892	.420	90	1.186	.739	90	1.486	1.034
95	.402	.201	95	.446	.210	95	.593	.369	95	.732	.517
100	.105	.105	100	0	0	100	0	0	100	0	0
Tangent point	80.00	60.00									
L.E. radius	0.0016c										
L.E. radius	0.0024c										
L.E. radius	0.0056c										
L.E. radius	0.0099c										



TABLE II  
SUMMARY OF STATIC LATERAL STABILITY DERIVATIVES

$\Lambda$ (deg)	t/c	Nacelle	$C_{Y\psi}$	$C_{n\psi}$	$C_{l\psi}$
10.8	0.04	Off	0.0012	0.00057	-0.00010
35	.04		.0018	.00046	0
47	.04		.0020	.00040	.00003
47	.06		.0022	.00030	-.00003
47	.09		.0026	.00017	-.00011
47	.06	On	.0076	.00122	-.00020
Body alone			.0015	.00055	.00004



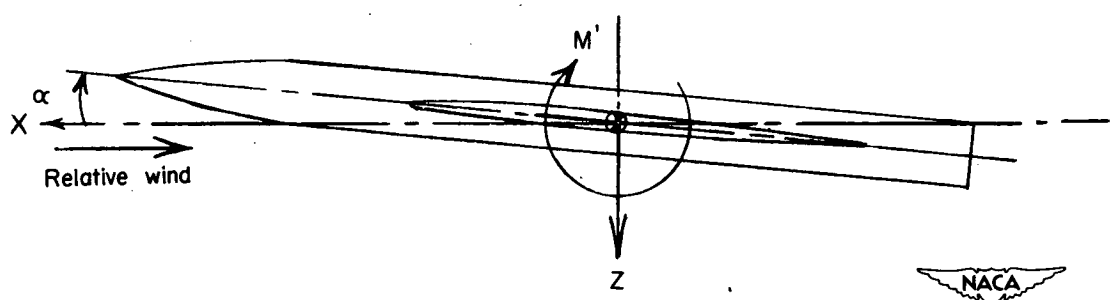
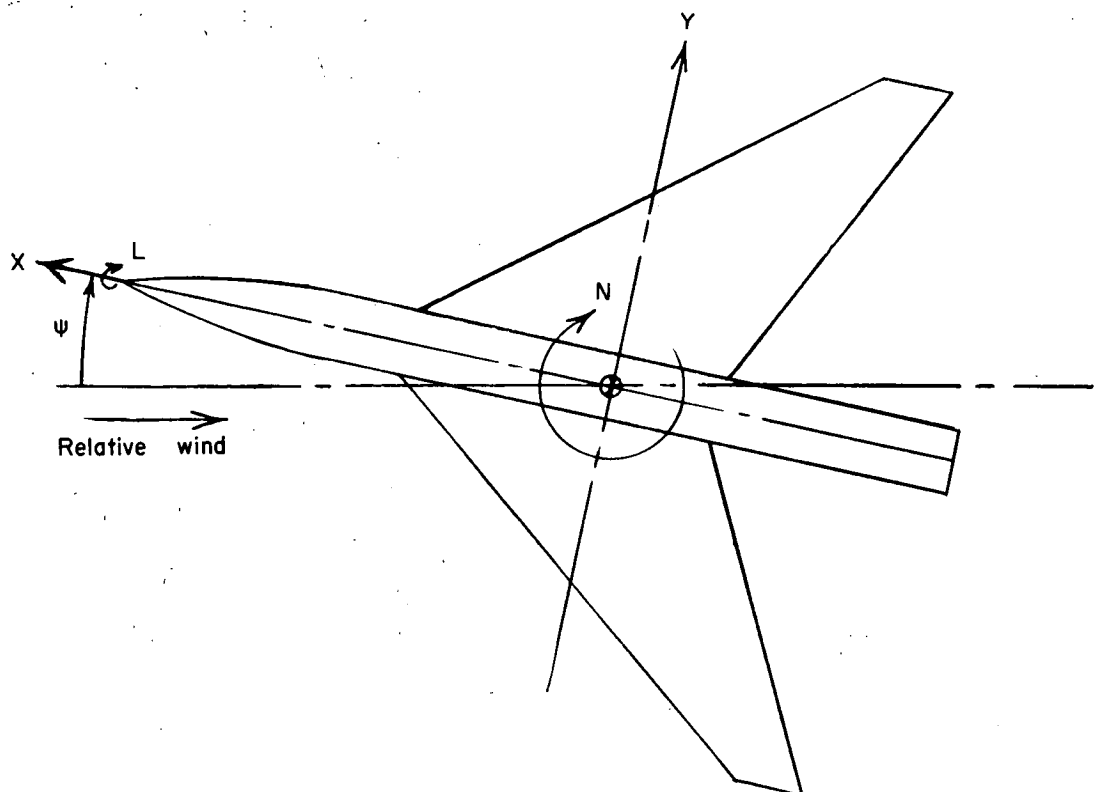
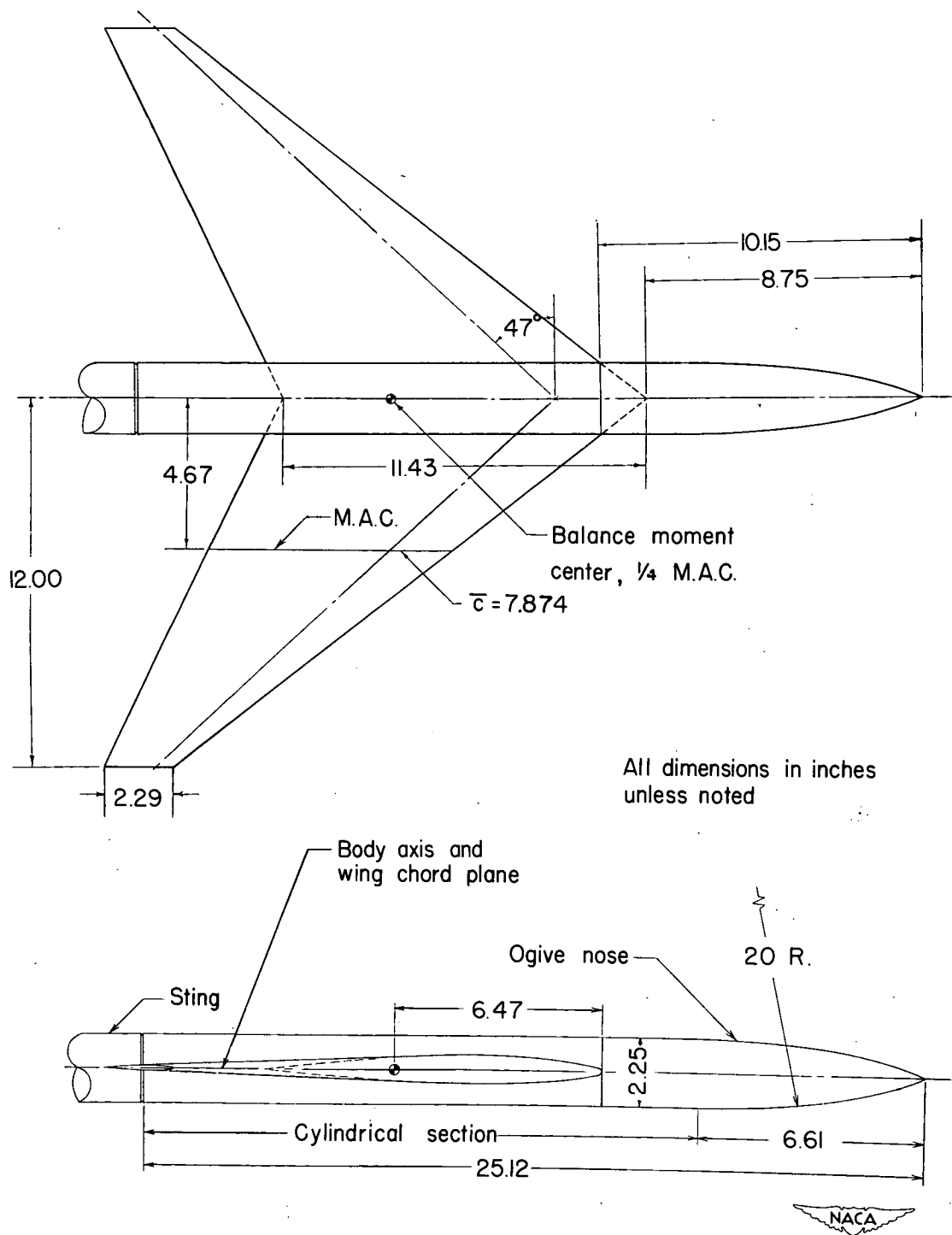


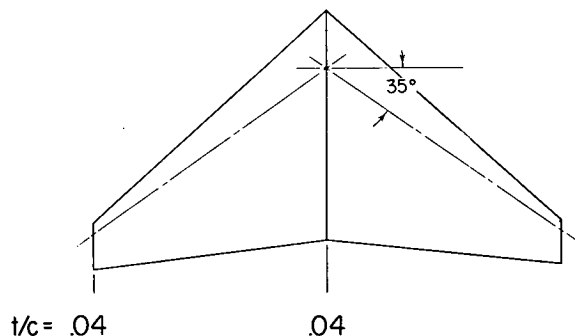
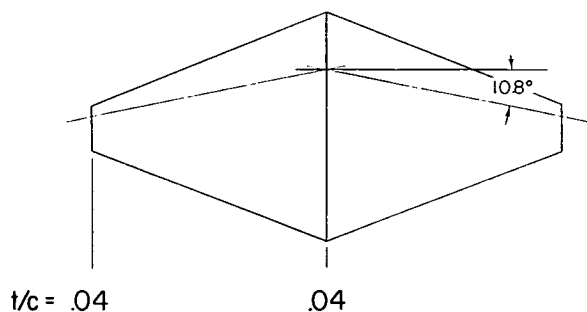
Figure 1.- System of stability axes. Arrows indicate positive values.



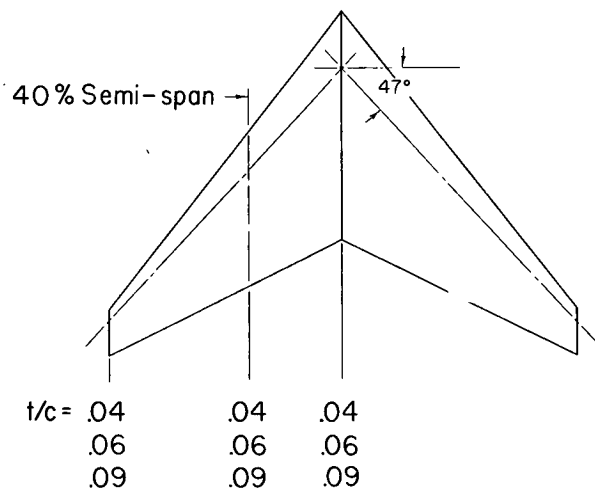


(a) Wing-body arrangement.

Figure 2.- Details of model configurations.

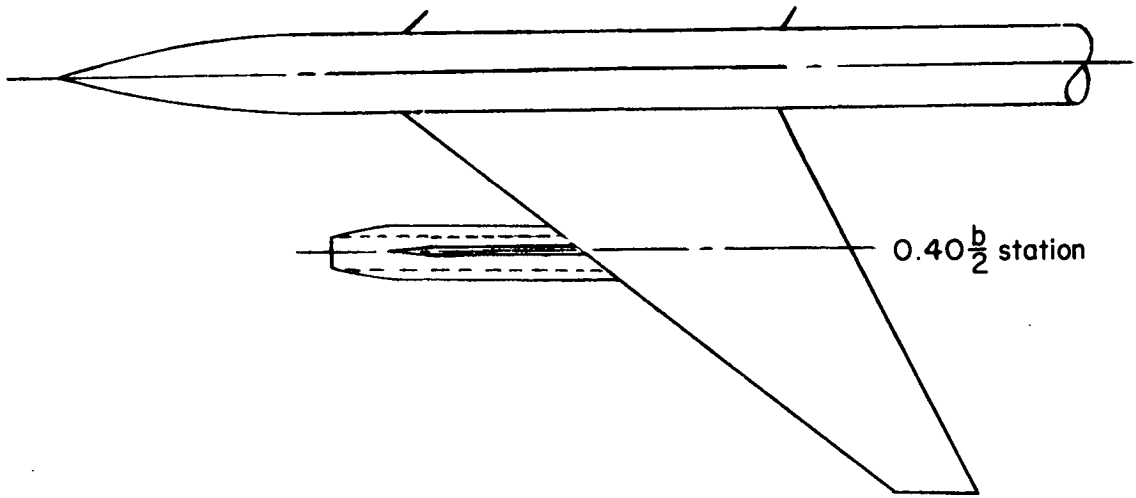


Aspect Ratio	3.5
Taper Ratio	0.2
Span, inches	24
Area, sq. feet	1143

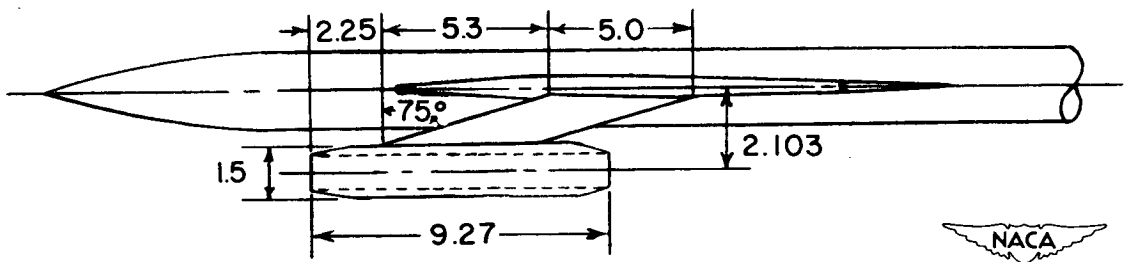


(b) Details of wings.

Figure 2.- Continued.

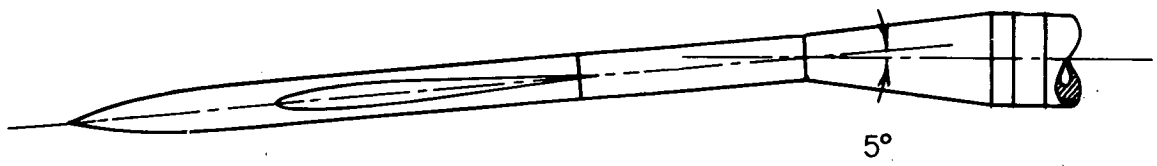


Strut section NACA 65<sub>A</sub> -005 in  
streamwise direction

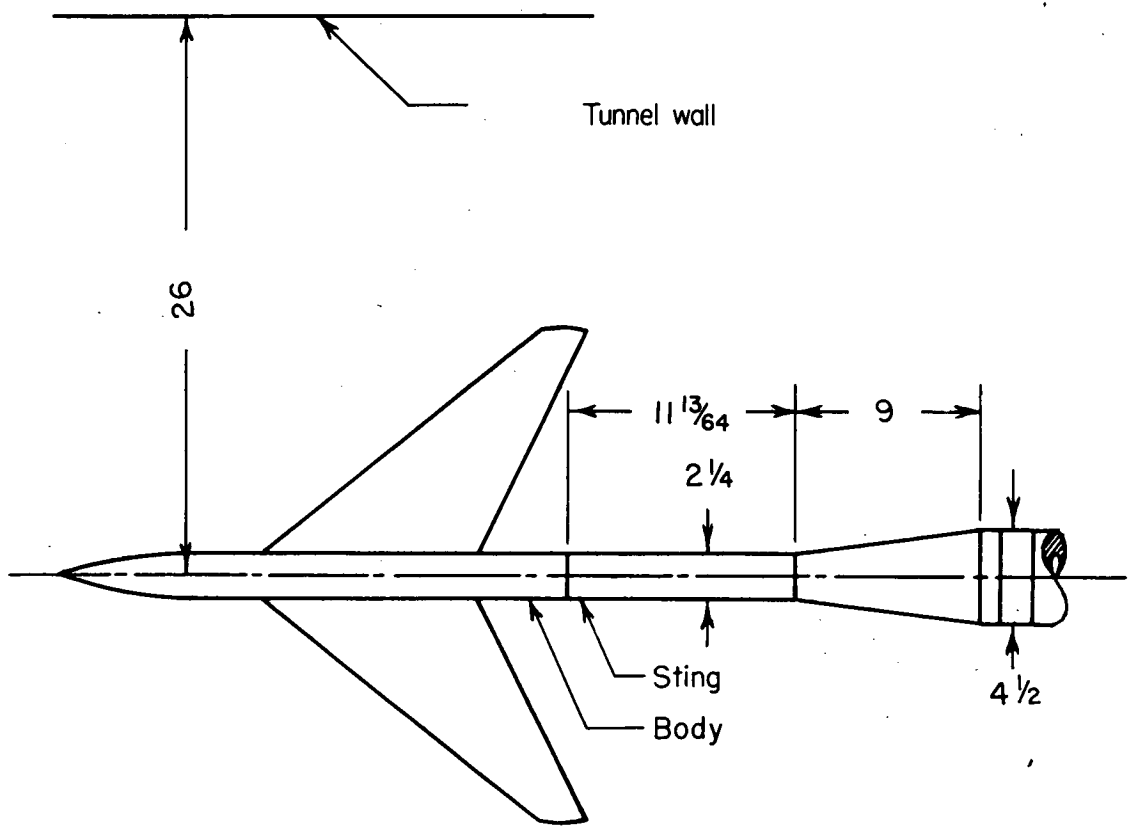


(c) Details of nacelle installation on  $\Lambda = 47^\circ$ ;  $\frac{t}{c} = 0.06$  wing.

Figure 2.- Concluded.



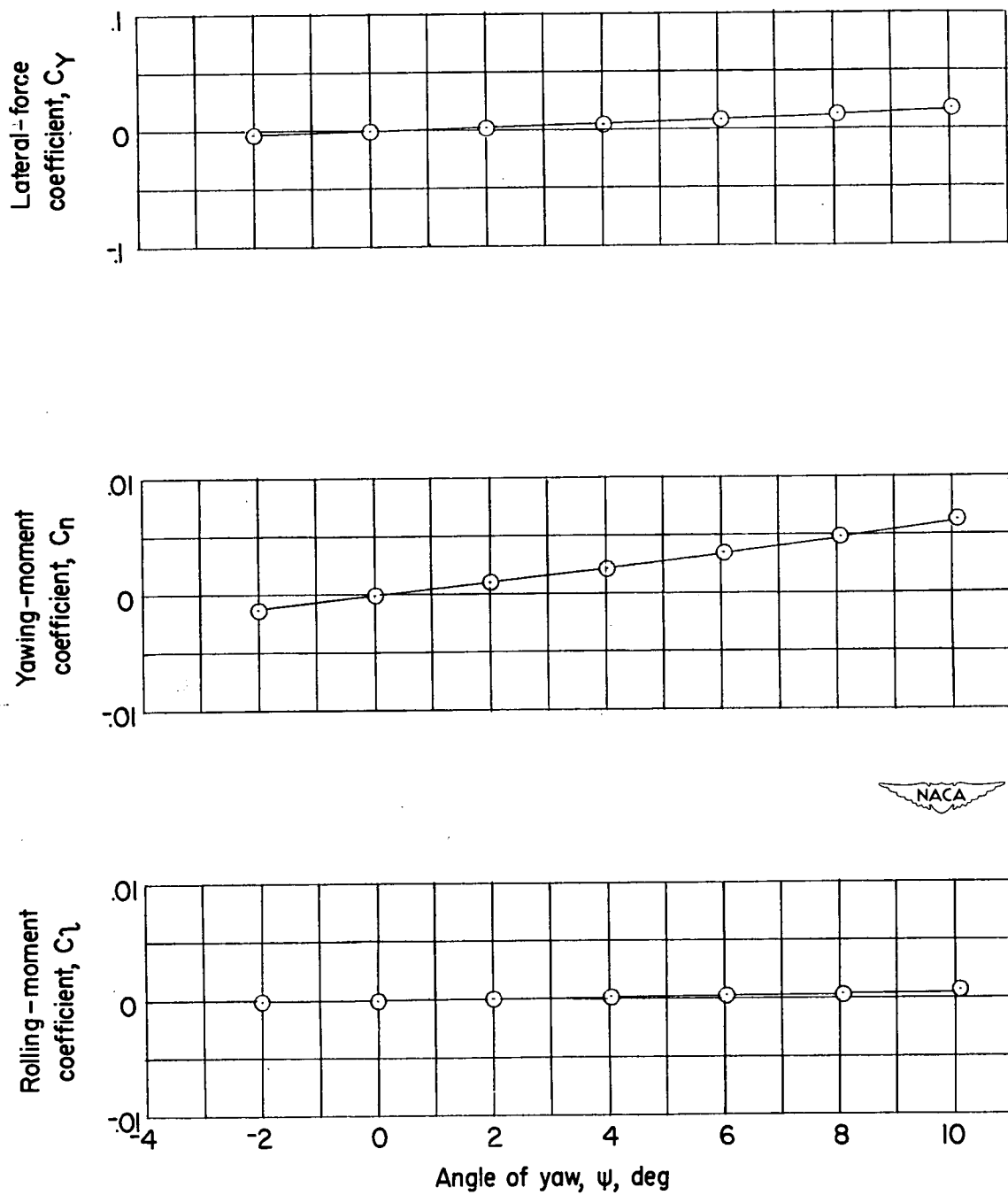
Top view of installation



Side view of installation

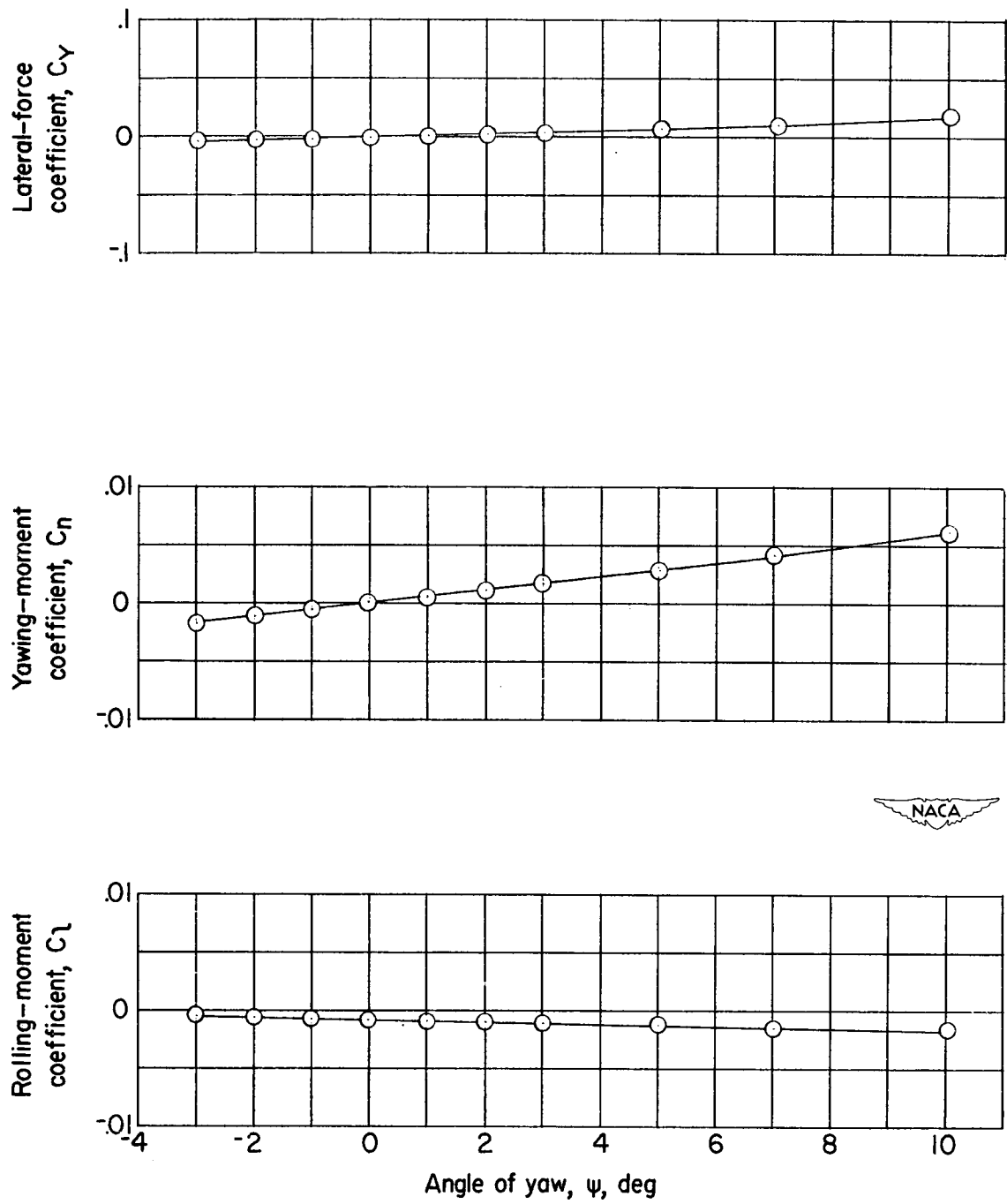


Figure 3.- Details of model sting support. All dimensions in inches unless noted.



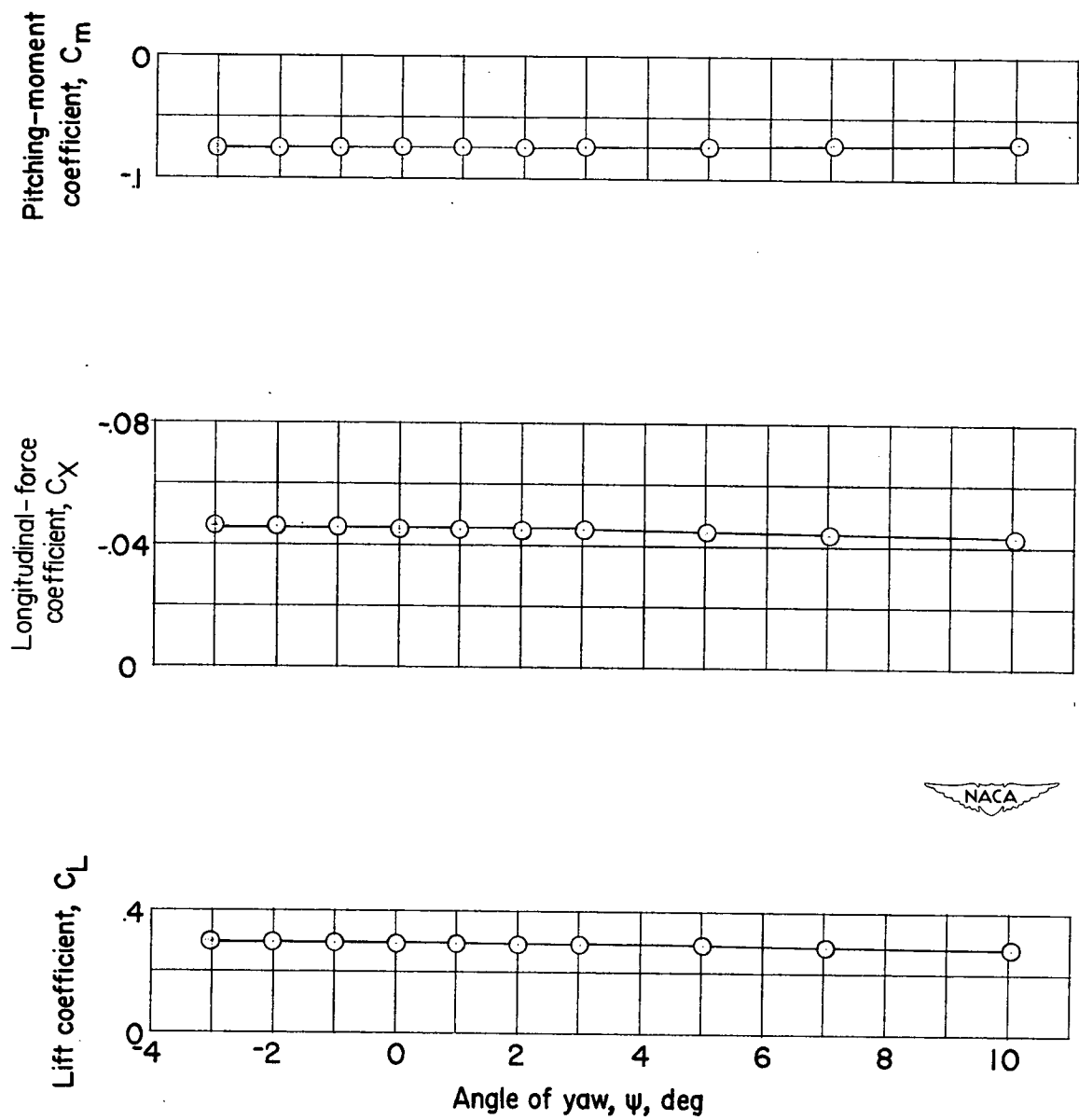
(a) Body alone.

Figure 4.- Aerodynamic characteristics in yaw for various configurations  
at  $\alpha = 5^\circ$ .  $M = 1.60$ .



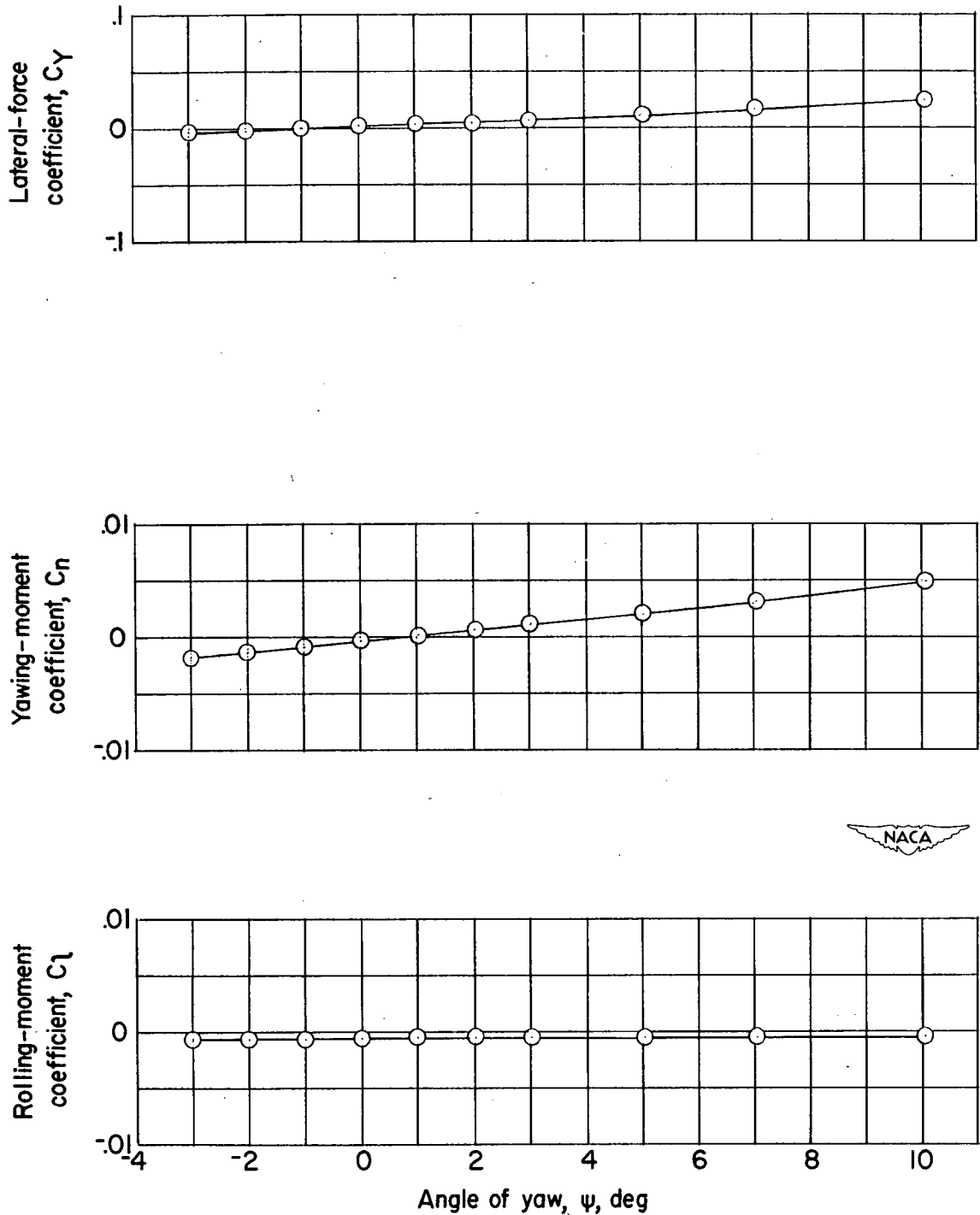
$$(b) \quad \Lambda = 10.8^\circ; \frac{t}{c} = 0.04.$$

Figure 4.- Continued.



(b) Concluded.

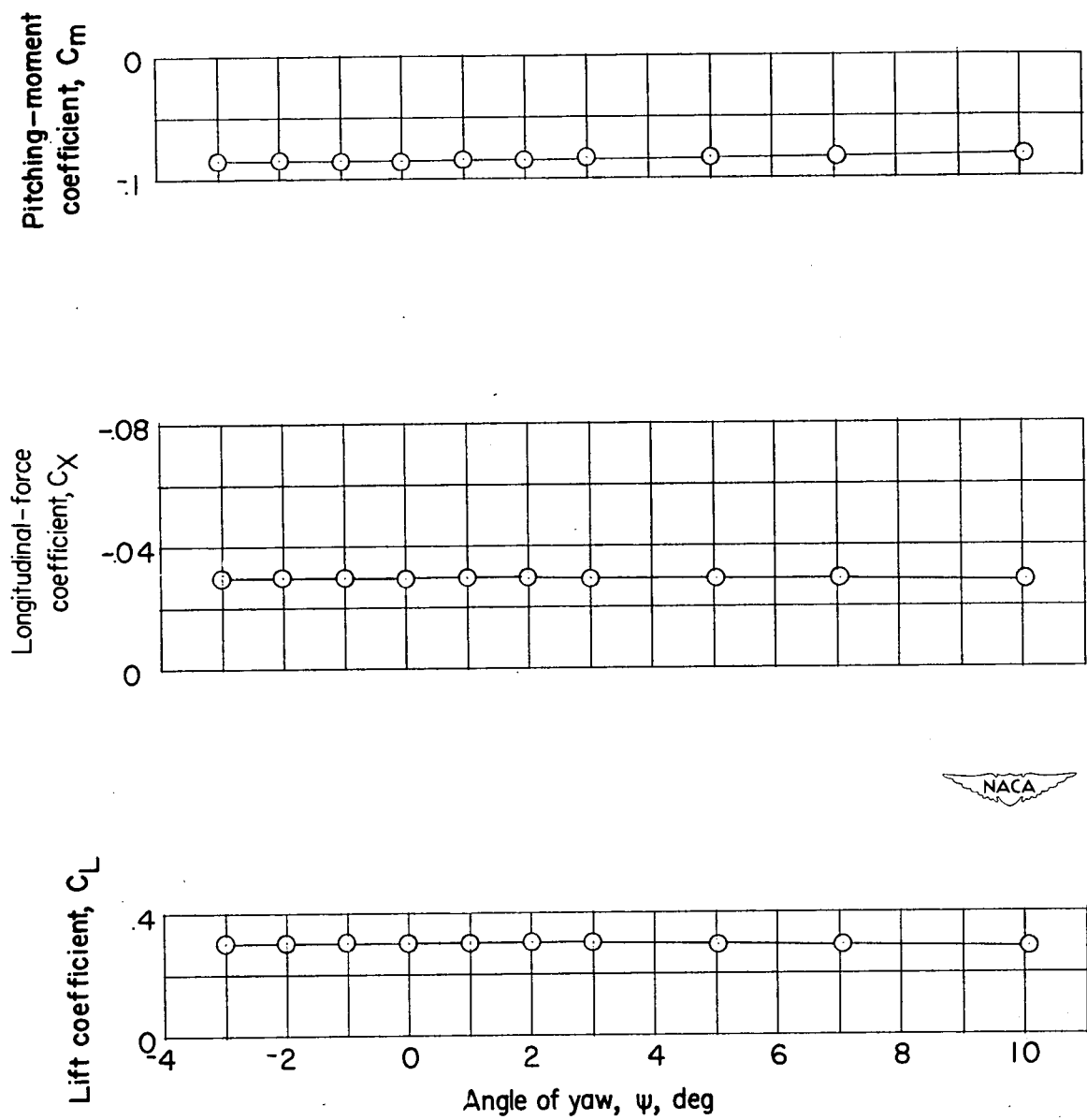
Figure 4.- Continued.



$$(c) \quad \Lambda = 35^\circ; \frac{t}{c} = 0.04.$$

Figure 4.- Continued.

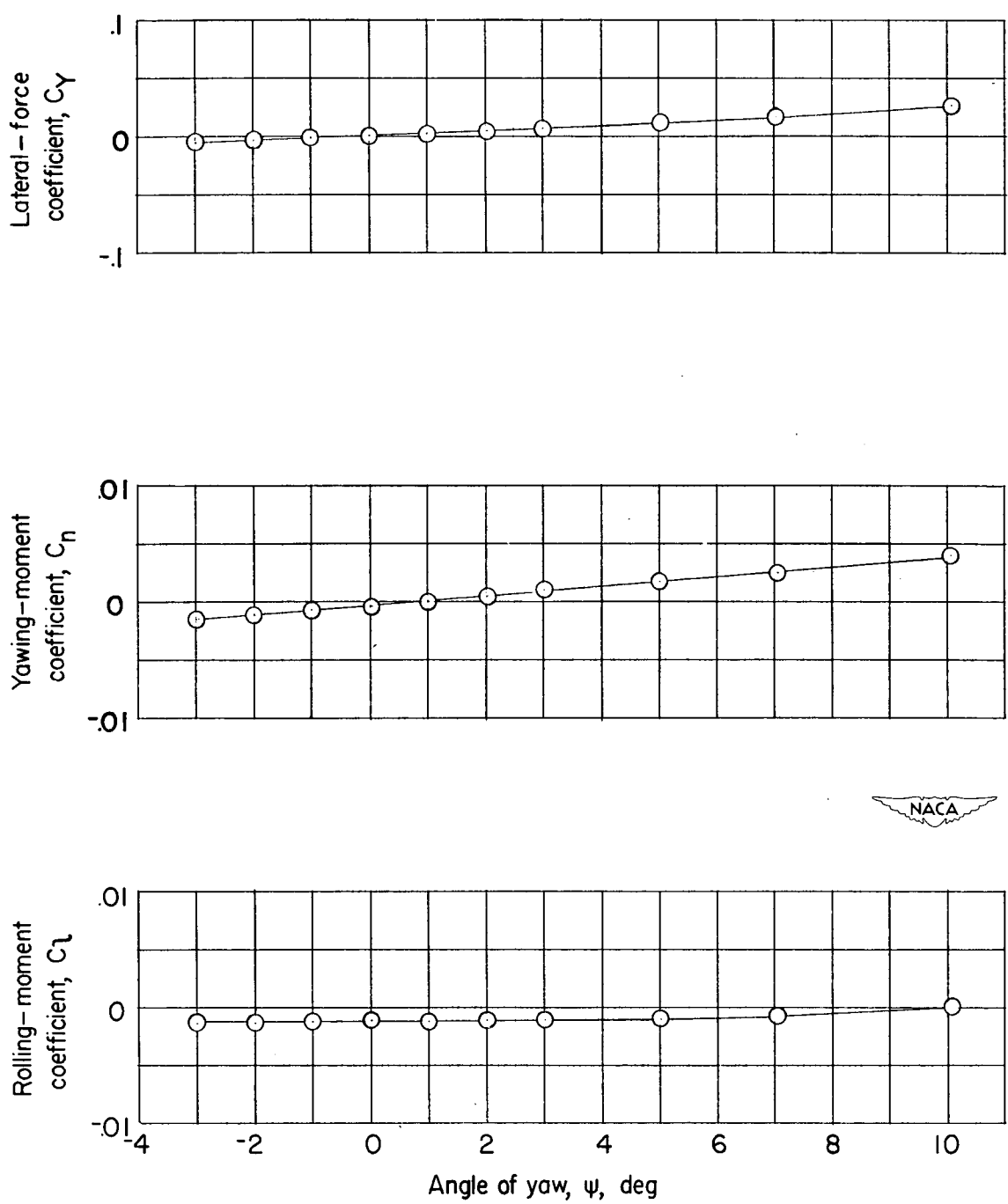




(c) Concluded.

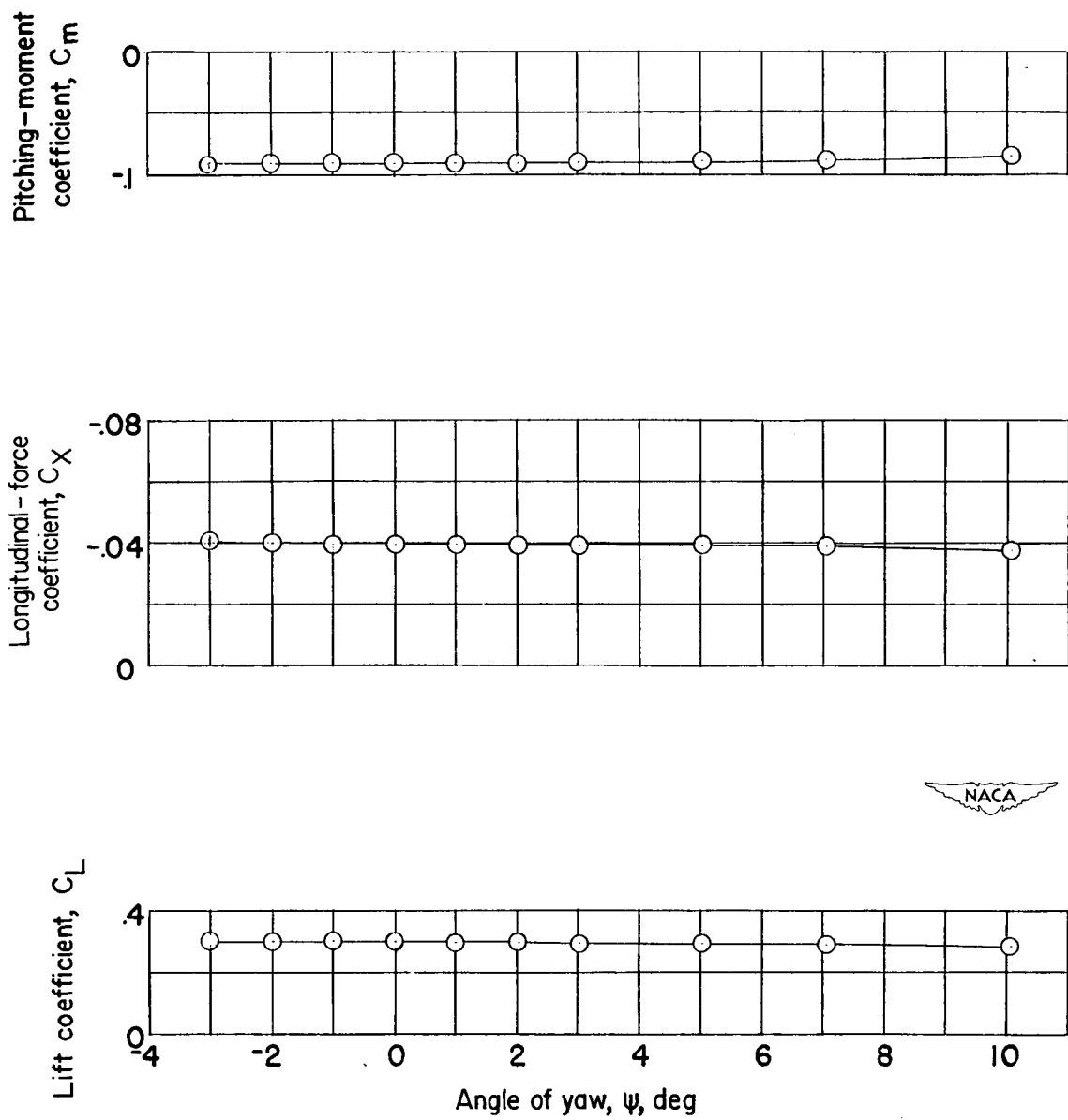
Figure 4.- Continued.





(d)  $\Delta = 47^\circ$ ;  $\frac{t}{c} = 0.04$ .

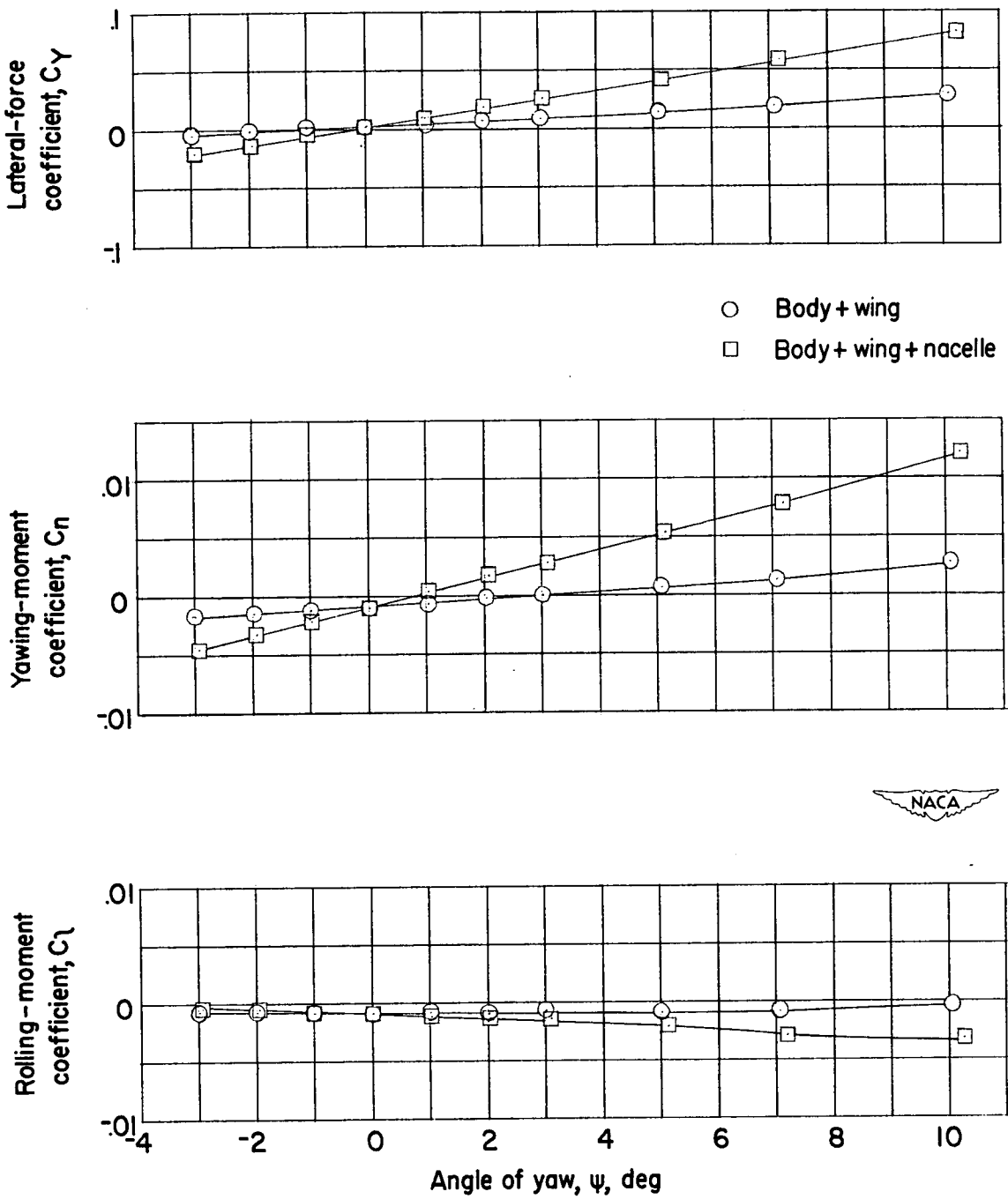
Figure 4.- Continued.



(d) Concluded.

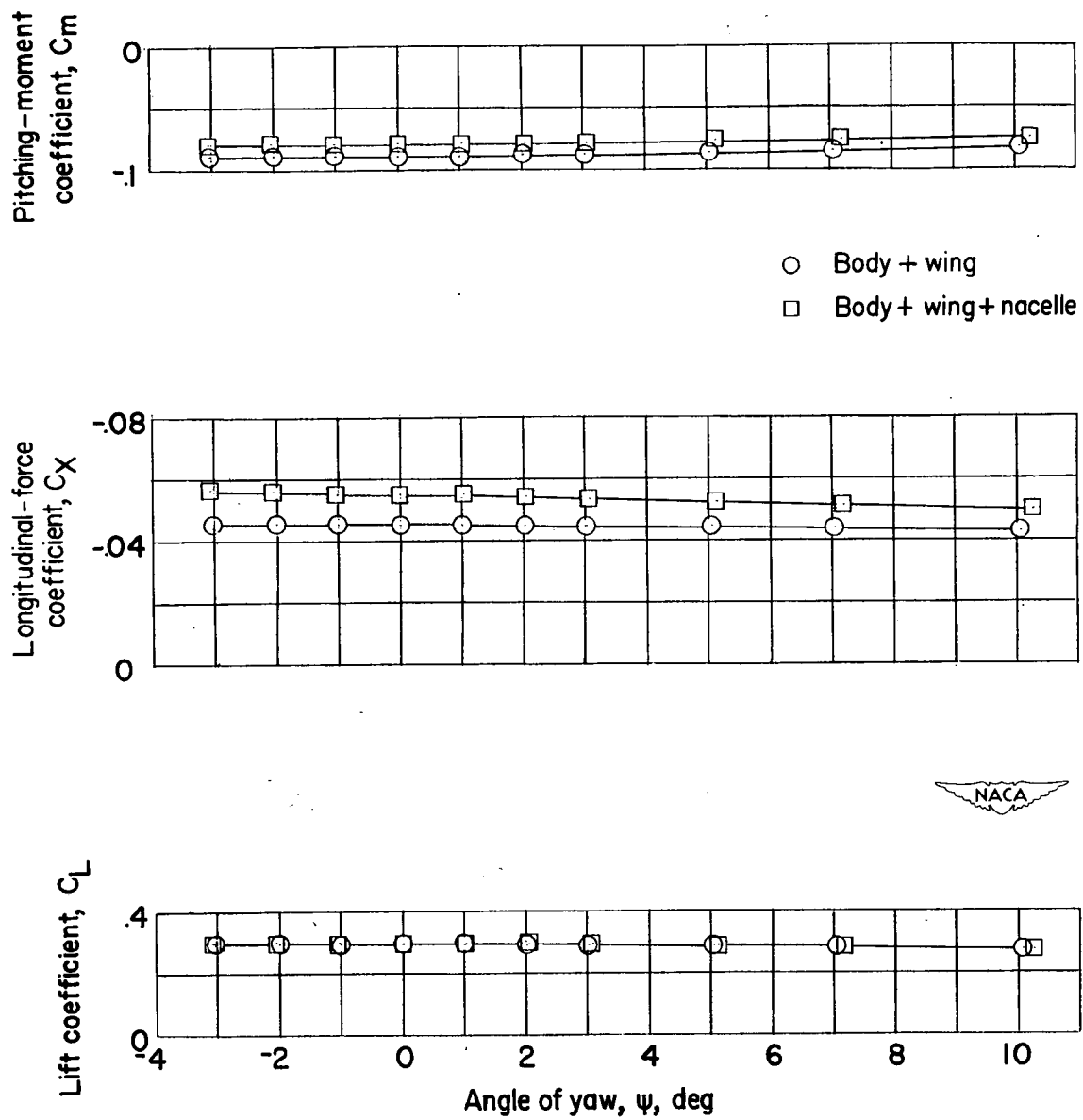
Figure 4.- Continued.





$$(e) \quad \Delta = 47^\circ; \quad \frac{t}{c} = 0.06.$$

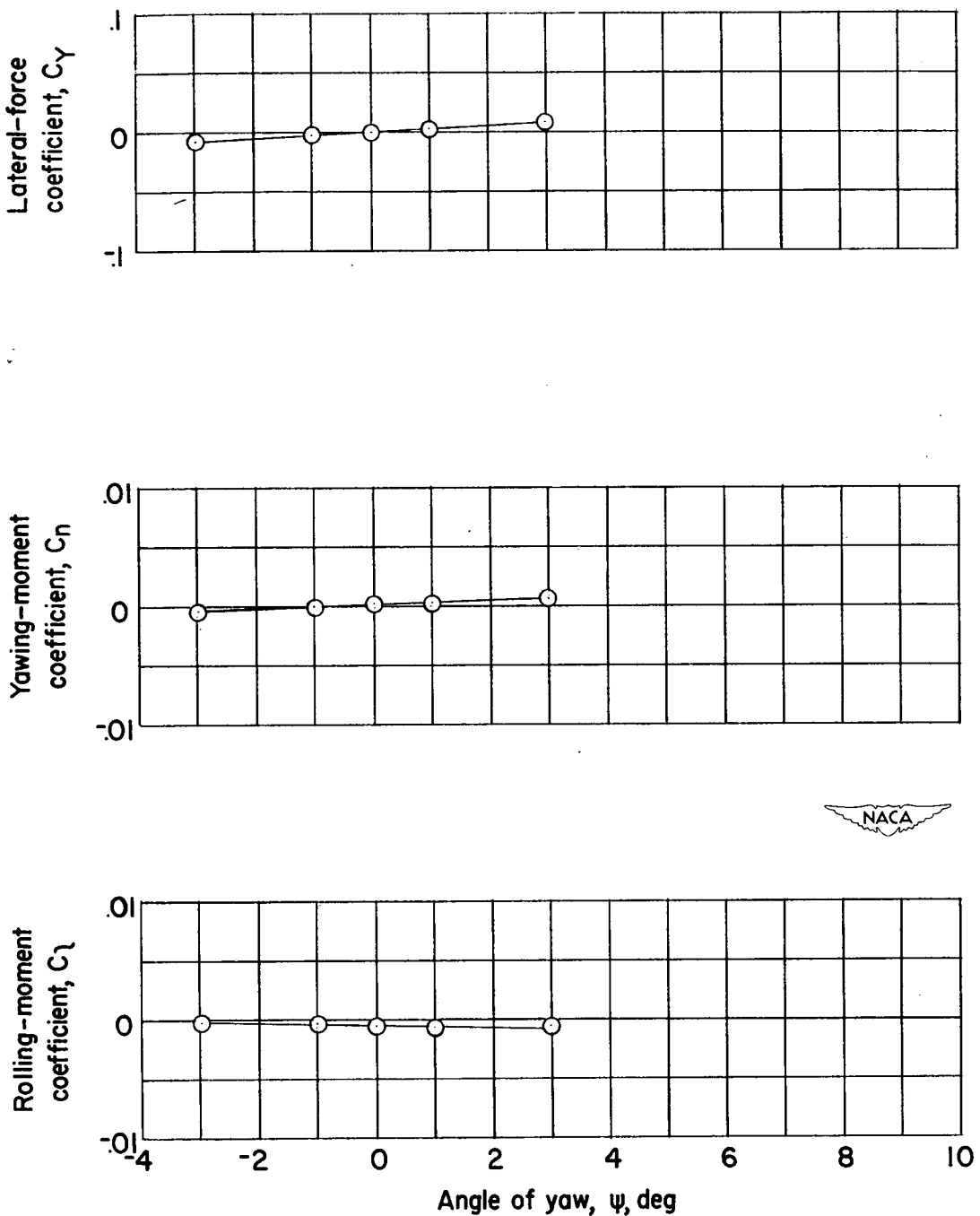
Figure 4.- Continued.



(e) Concluded.

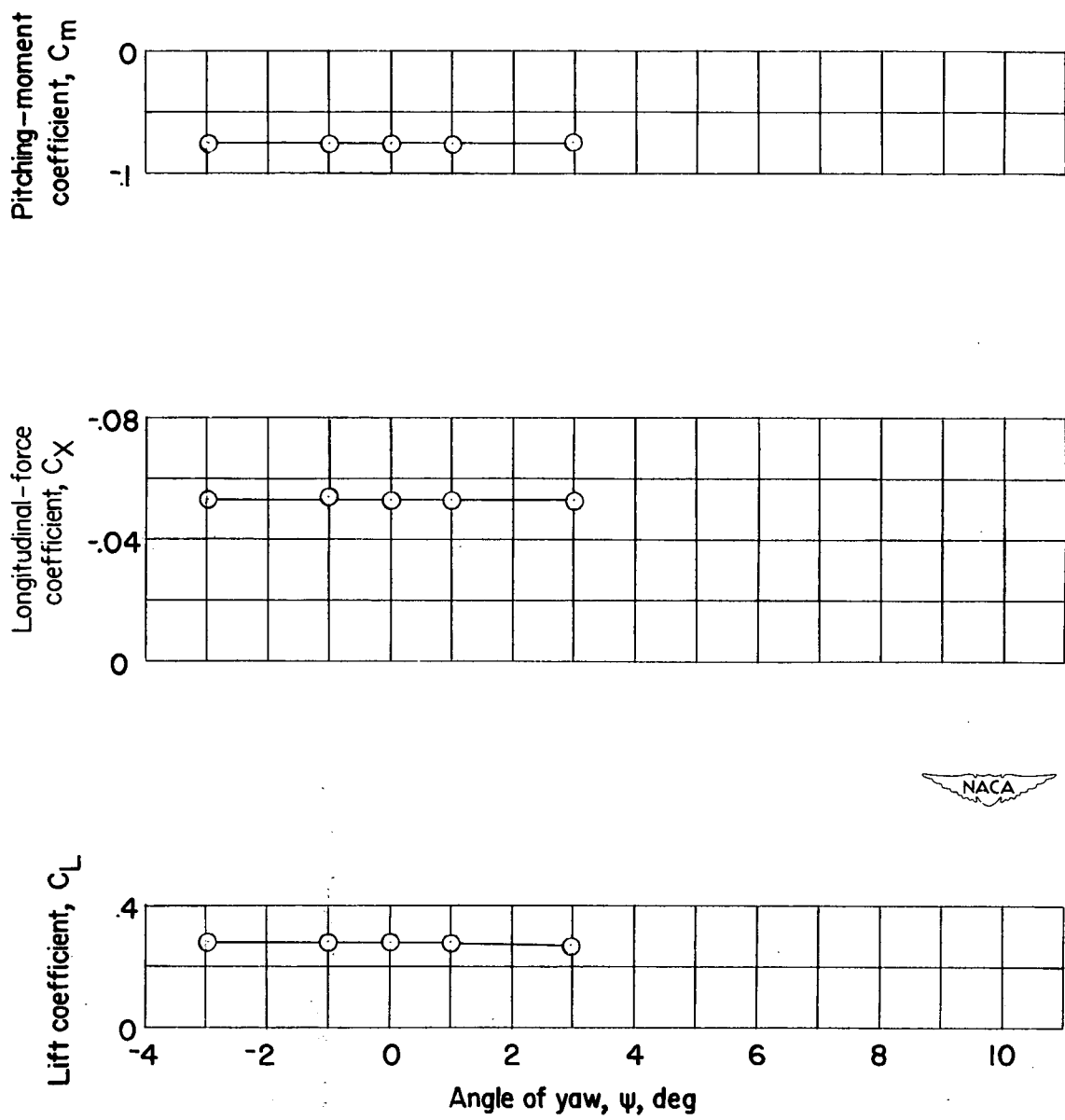
Figure 4.- Continued.





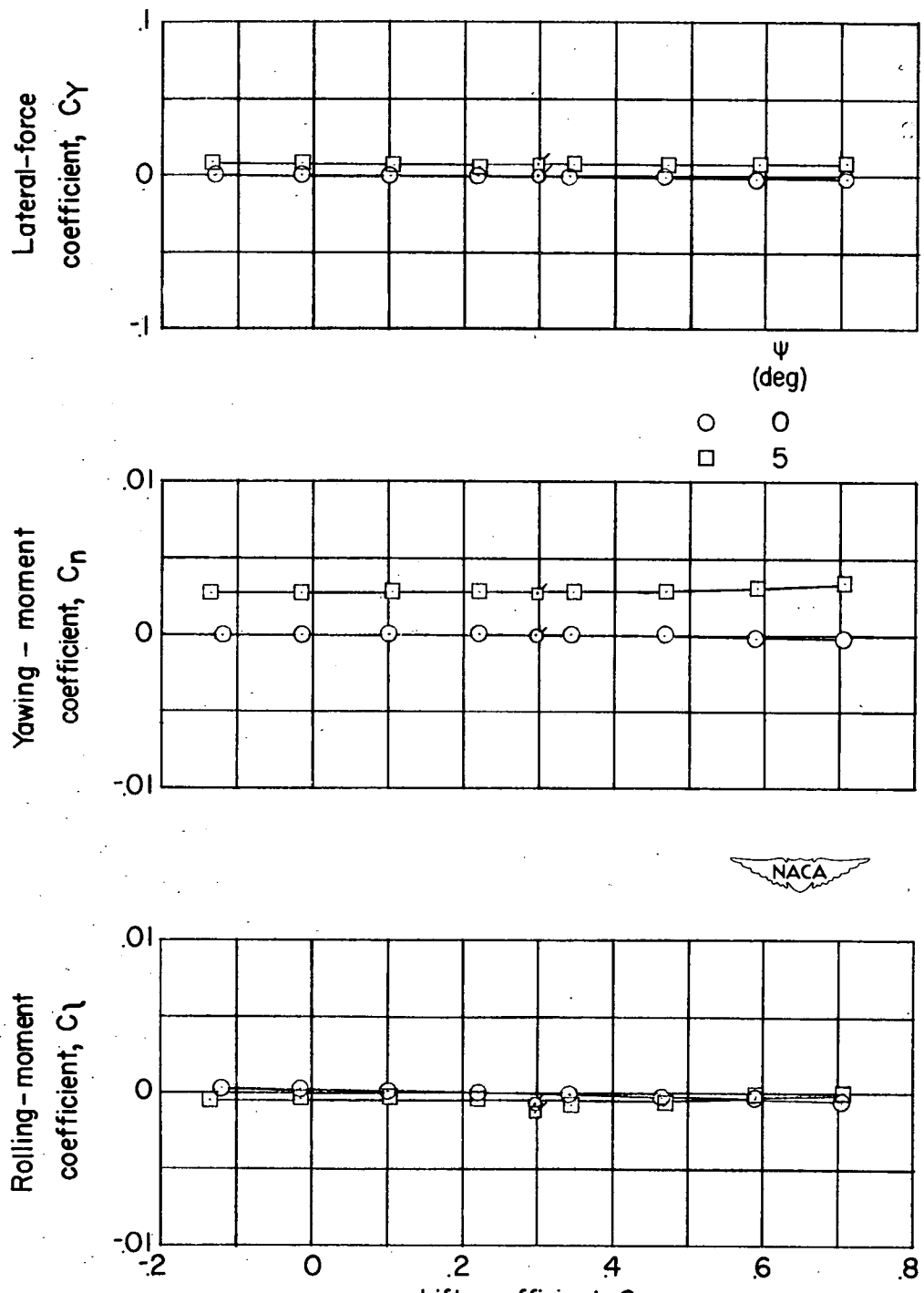
$$(f) \quad \Lambda = 47^\circ; \frac{t}{c} = 0.09.$$

Figure 4.- Continued.



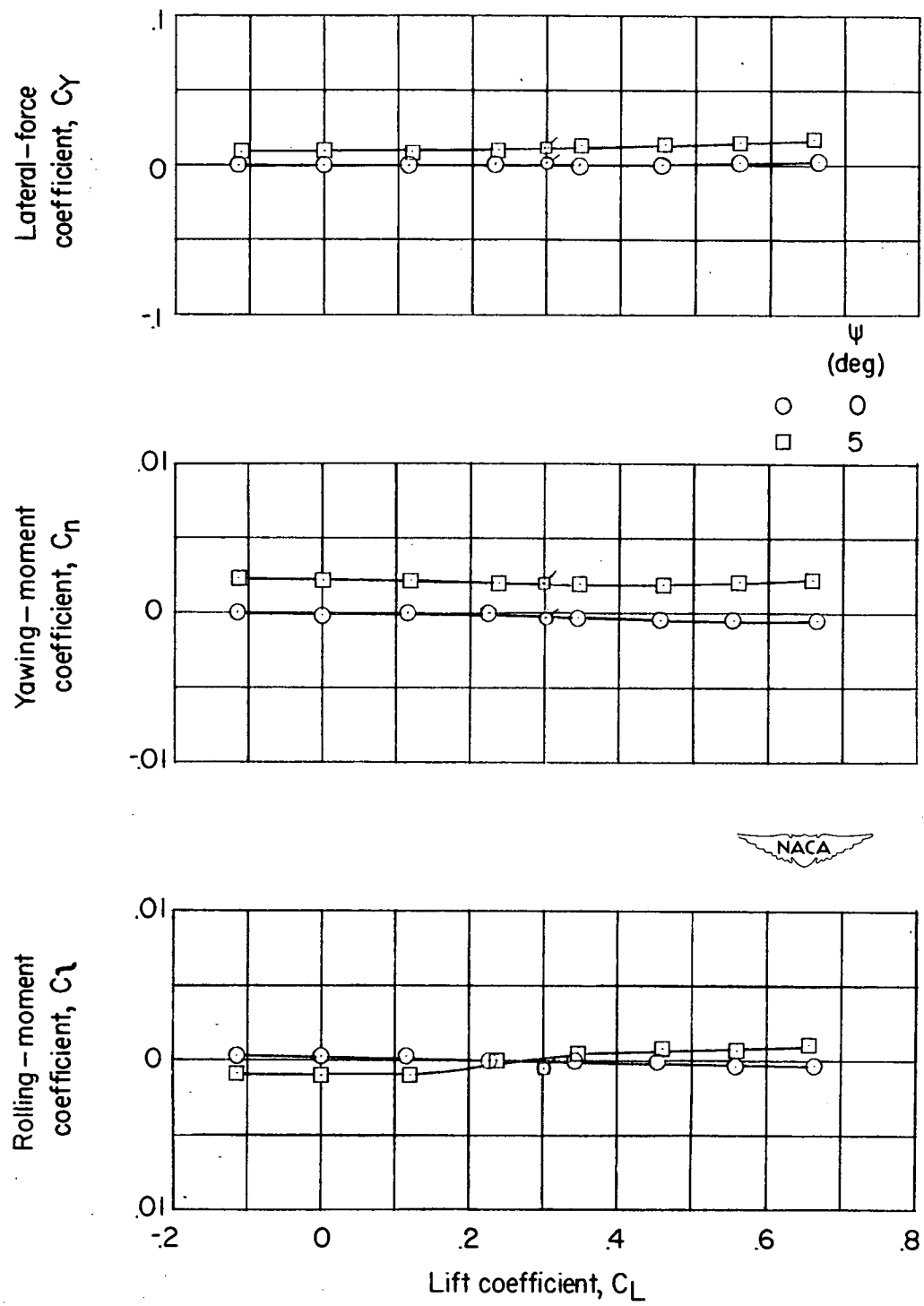
(f) Concluded.

Figure 4.- Concluded.



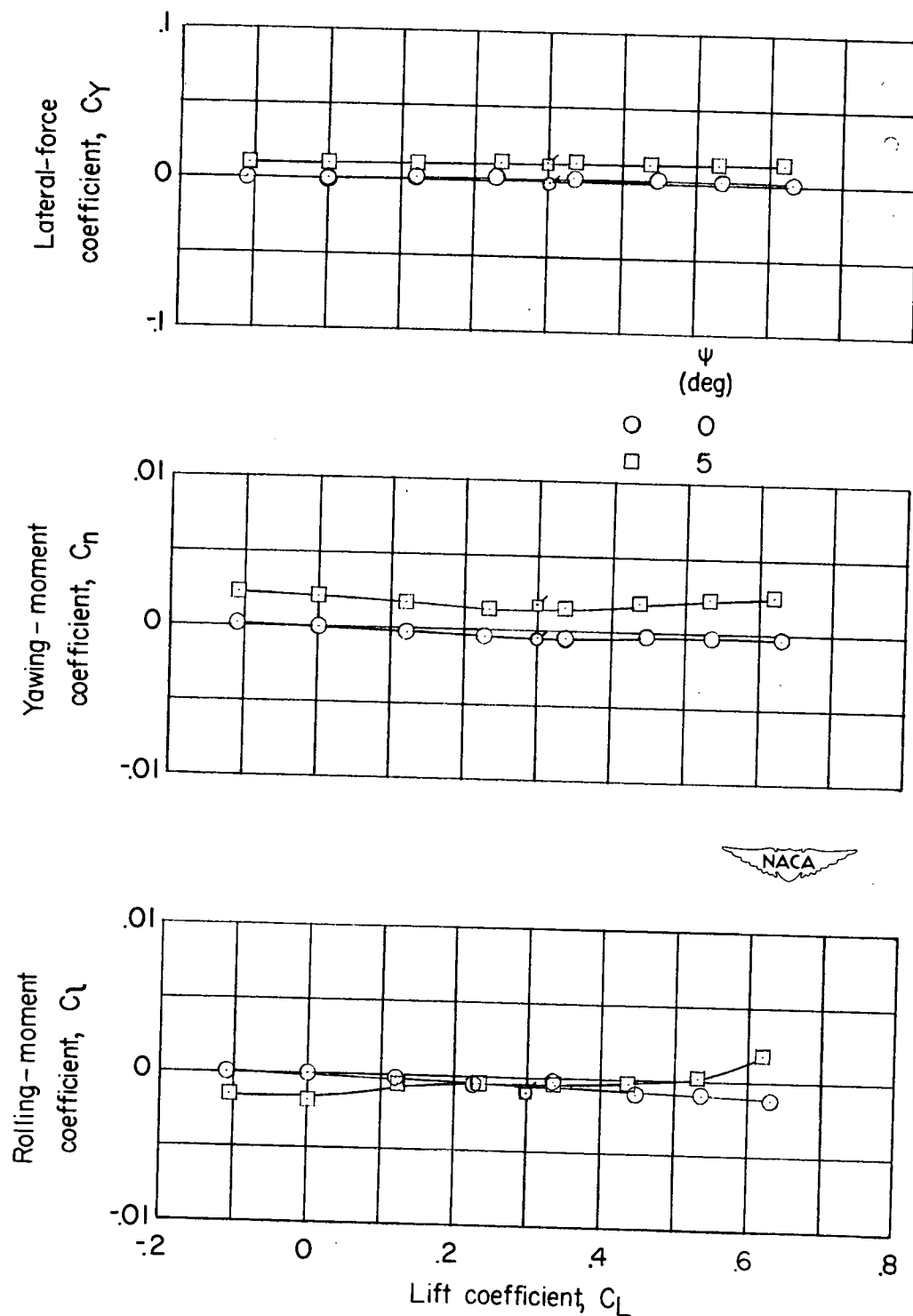
$$(a) \quad \Lambda = 10.8^\circ; \quad \frac{t}{c} = 0.04.$$

Figure 5.- Effect of yaw on the lateral characteristics in pitch for various configurations. Flagged symbols are values from yaw tests.



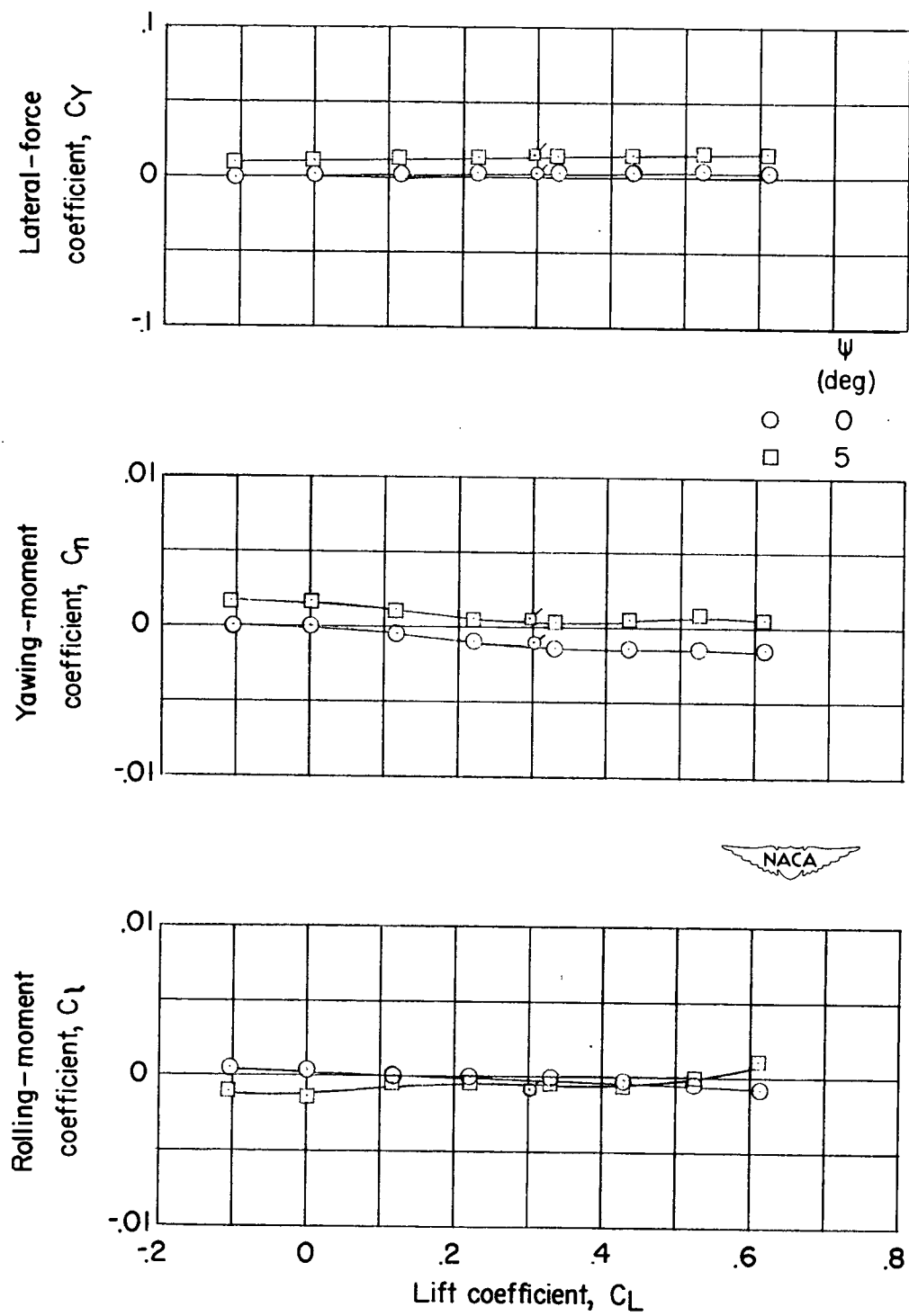
(b)  $\Delta = 35^\circ$ ;  $\frac{t}{c} = 0.04$ .

Figure 5.- Continued.



(c)  $\Lambda = 47^\circ$ ;  $\frac{t}{c} = 0.04$ .

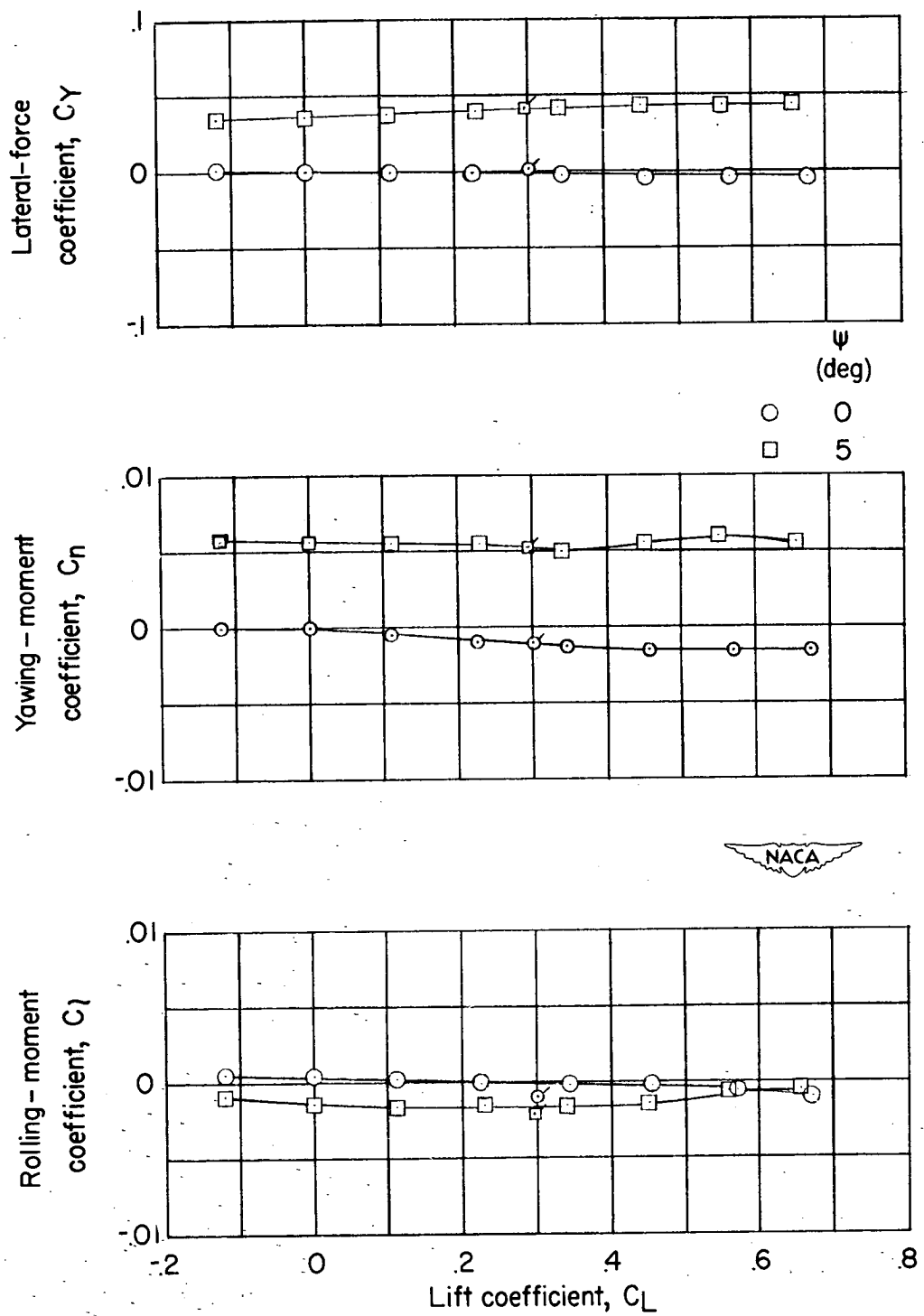
Figure 5.- Continued.



$$(d) \quad \Lambda = 47^\circ; \quad \frac{t}{c} = 0.06.$$

Figure 5.- Continued.





(e)  $\Lambda = 47^\circ$ ;  $\frac{t}{c} = 0.06$ , nacelle on.

Figure 5.- Concluded.

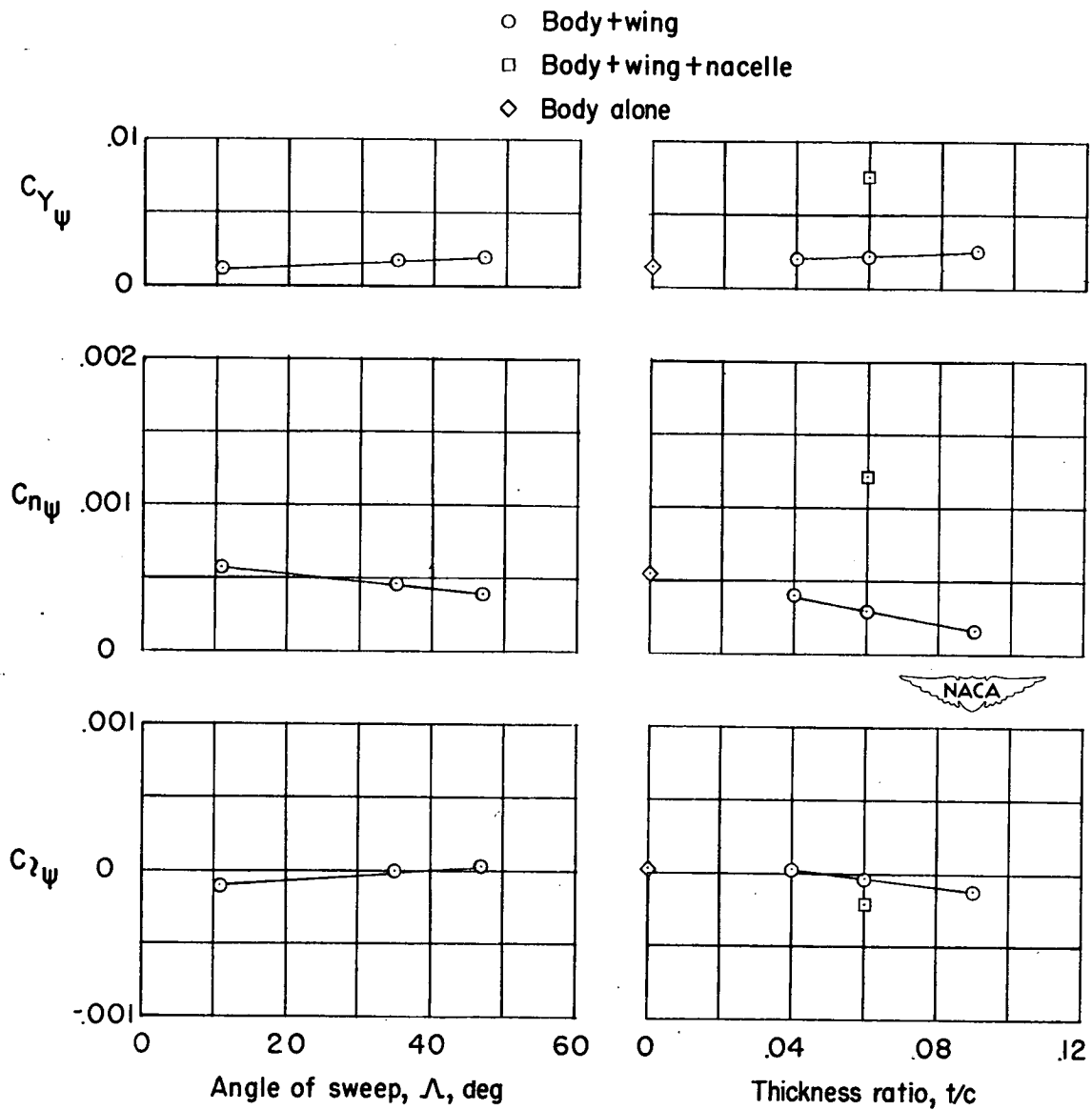


Figure 6.- Summary of the static lateral stability characteristics of various configurations at  $\alpha = 5^\circ$ .  $M = 1.60$ .